Lateral Heterogeneity of Dipalmitoylphosphatidylethanolamine−Cholesterol Langmuir−Blodgett Films Investigated with Imaging Time-of-Flight Secondary Ion Mass Spectrometry and Atomic Force Microscopy

Carolyn M. McQuaw, Audra G. Sostarecz, Leiliang Zheng, Andrew G. Ewing, and Nicholas Winograd*

Department of Chemistry, The Pennsylvania State University, 104 Chemistry Building, University Park, Pennsylvania 16802

Received August 17, 2004. In Final Form: October 22, 2004

To better understand the influence of cholesterol (CH) on dipalmitoylphosphatidylethanolamine (DPPE), Langmuir−Blodgett (LB) model membranes of DPPE with varying amounts of cholesterol were imaged by time-of-flight secondary ion mass spectrometry (ToF-SIMS) and atomic force microscopy (AFM). Cholesterol has a condensing effect on DPPE that at low cholesterol concentrations results in lateral heterogeneity of the LB monolayer. At 4:1 DPPE/CH, islands of DPPE/CH phase exist with a connected DPPE phase. As the concentration of cholesterol is increased, the percolation threshold is crossed and the DPPE/CH phase islands connect to separate the DPPE phase (2:1 DPPE/CH). Finally, at 50 mol % cholesterol a single homogeneous DPPE/CH phase LB monolayer exists. ToF-SIMS of the DPPE/CH phase provides a lower ion signal for the characteristic lipid fragments and substrate apparently owing to the higher molecular density induced by cholesterol. AFM data indicate that the DPPE/CH phase is lower in height than the DPPE phase. As phosphatidylethanolamine is predominant in the inner lipid leaflet of cellular membranes, this work has implications for the understanding of cholesterol domains in the inner leaflet of cells.

Introduction

Understanding the factors that influence the formation of cholesterol domains within the lipid bilayer is of significant interest due to their proposed participation in transport and signaling in cellular membranes.[1] The phospholipids in these domains are expected to be in a liquid-ordered (l_o) phase that is characterized by tightly packed chains and a high degree of lateral mobility.[1] The complexity of cellular membranes magnifies the difficulty in investigating the factors that influence the formation of cholesterol domains. Model membrane systems, such as those made using the Langmuir−Blodgett (LB) technique, are useful in decreasing the complexity by creating well-defined, reproducible membrane mimics.

In this study, LB membrane models of inner plasma membrane bilayer lipids are used to investigate lipid interactions and the formation of micrometer-size cholesterol-rich domains. Dipalmitoylphosphatidylethanolamine (DPPE) was chosen because phosphatidylethanolamine phospholipids are the most abundant lipids in the inner leaflet of the plasma membrane, and cholesterol (CH) was selected due to its essential role in the formation of lipid domains. We recently showed that cholesterol domain formation is possible in a phosphatidylethanolamine-rich environment.[2] The data presented here are an in-depth look at their formation.

Lipid LB model membranes are typically investigated using fluorescence microscopy or atomic force microscopy (AFM).[3−7] Both techniques provide detection of lateral lipid heterogeneity; however these techniques are limited in that stepwise experiments or fluorescent dyes are necessary to chemically identify the phases. One novel method used to interrogate LB model membrane systems that does not require stepwise experiments or fluorescent dyes is time-of-flight secondary ion mass spectrometry (ToF-SIMS).[2,8−12] This technique, due to its high surface sensitivity and imaging capabilities, allows chemical determination of the lateral distributions of lipids in LB monolayers.

In this report, we analyze LB model membranes of DPPE and cholesterol using both ToF-SIMS and AFM. Our monolayer studies at the air−water interface show that cholesterol has a condensing effect on DPPE that produces lateral heterogeneity in the LB monolayer at low cholesterol concentrations. In the 4:1 DPPE/CH monolayer, the cholesterol forms islands of DPPE/CH in a connected DPPE phase. As the concentration of cholesterol is increased, the percolation threshold is crossed and the DPPE/CH islands connect to separate the DPPE phase. Then at 50 mol % cholesterol a single homogeneous liquid phase of DPPE and cholesterol exists. The addition of cholesterol increases the molecular density of the monolayer that leads to lower lipid characteristic ion and

* To whom correspondence should be addressed. Telephone: (814) 865-0493. Fax: (814) 863-0618. E-mail: nxw@psu.edu.

(1) Brown, D. A.; London, E. *J. Membr. Biol.* **1998**, *164*, 103−114.
(2) Sostarecz, A. G.; McQuaw, C. M.; Ewing, A. G.; Winograd, N. *J. Am. Chem. Soc.* **2004**, *126*, 13882−13883.
(3) Slotte, J. P. *Biochim. Biophys. Acta* **1995**, *1235*, 419−427.
(4) Slotte, J. P. *Biochim. Biophys. Acta* **1995**, *1238*, 118−126.
(5) Slotte, J. P.; Mattjus, P. *Biochim. Biophys. Acta* **1995**, *1254*, 22−29.
(6) Yuan, C.; Johnston, L. J. *Biophys. J.* **2000**, *79*, 2768−2781.
(7) Yuan, C.; Johnston, L. J. *J. Microsc.* **2002**, *205*, 136−146.
(8) Biesinger, M. C.; Paepegaey, P.-Y.; McIntyre, N. S.; Harbottle, R. R.; Petersen, N. O. *Anal. Chem.* **2002**, *74*, 5711−5716.
(9) Bourdos, N.; Kollmer, F.; Benninghoven, A.; Ross, M.; Sieber, M.; Galla, H.-J. *Biophys. J.* **2000**, *79*, 357−369.
(10) Harbottle, R. R.; Nag, K.; McIntyre, N. S.; Possmayer, F.; Petersen, N. O. *Langmuir* **2003**, *19*, 3698−3704.
(11) Ross, M.; Steinem, C.; Galla, H.-J.; Janshoff, A. *Langmuir* **2001**, *17*, 2437−2445.
(12) Sostarecz, A. G.; Cannon, D. M., Jr.; McQuaw, C. M.; Sun, S.; Ewing, A. G.; Winograd, N. *Langmuir* **2004**, *20*, 4926−4932.

10.1021/la0479455 CCC: $30.25
Published on Web 00/00/0000 PAGE EST: 6.1

substrate signals in ToF-SIMS spectra. AFM has been used to determine that the cholesterol-rich phase in the heterogeneous films is lower in height than the DPPE phase. This study is unique in that it examines the influence of increasing cholesterol concentration on a phospholipid monolayer by chemically identifying the lateral distribution of the lipids. We have shown that DPPE and cholesterol interact to form a DPPE/CH phase and that the formation of cholesterol domains in the phosphatidylethanolamine-rich inner bilayer leaflet is possible. This is significant because mechanisms of signaling and transport across a lipid bilayer that are dependent on domain structures will require the existence of cholesterol domains in both leaflets.

Materials and Methods

Materials. The following chemicals were used without further purification: 16-mercaptohexadecanoic acid (Sigma-Aldrich Co., St. Louis, MO), 2-propanol, methanol, chloroform, DPPE, and cholesterol (both lipids were from Avanti Polar Lipids, Inc., Alabaster, AL). A Milli-Q system (Millipore, Burlington, MA) was used to purify the water necessary for the production of all LB films. The final resistivity of the water was 18.2 MΩ cm with a total organic content of less than 5 ppb.

Substrate Preparation. Self-assembled monolayers (SAMs) on gold were used as the LB substrates. The 3 in. single-crystal (100) silicon wafers used were piranha etched (3:1 H_2SO_4/H_2O_2) before Au deposition. (Extreme caution must be exercised when using piranha etch. An explosion-proof hood should be used.) After etching, the silicon substrates were then deposited with chromium and Au as described by Fisher et al.[13] A 1 mM solution of 16-mercaptohexadecanoic acid in 2-propanol was used for formation of the SAMs onto the gold substrates. SAM self-assembly and LB film deposition were confirmed with a single-wavelength (632.8 nm, 1 mm spot size, 70° incidence angle) Stokes ellipsometer LSE (Gaertner Scientific Corp., Skokie, IL).

Langmuir−Blodgett Film Preparation and Analysis. A Kibron μTrough S-LB (Helsinki, Finland) was used to prepare the LB films. The subphase was ~65 mL room-temperature Millipore purified water. All lipid mixtures were dissolved in 9:1 chloroform/methanol except for pure cholesterol which was dissolved in 3:2 hexane/2-propanol. At least 10 min was allotted before compression to allow for solvent evaporation and film equilibration. The surface pressure was measured with a Wilhelmy wire interfaced to a personal computer. Uniform compression (7 Å²/molecule/min) of the lipid layer was ensured through computer control of the trough barriers, and this also allowed for constant feedback during deposition to the substrate. The 4:1, 2:1, and 1:1 DPPE/CH films were each deposited vertically at a rate of 3 mm/min onto SAM substrates at 3 mN/m upon first compression. Although higher pressures are believed to mimic biological membrane densities, lower pressures are required to investigate lipid miscibility.[14]

To quantify the influence of cholesterol on DPPE, the average molecular area of an ideal mixture ($A'_{DPPE/CH}$) at 3 mN/m is compared to the actual molecular area observed ($A_{DPPE/CH}$). $A'_{DPPE/CH}$ is the molecular area expected for a noninteracting, immiscible mixture.[15] $A'_{DPPE/CH}$ is calculated by the following equation:

$$A'_{DPPE/CH} = X_{DPPE}A_{DPPE} + X_{CH}A_{CH} \quad (1)$$

where X_{DPPE} is the mole fraction of DPPE in the mixture, A_{DPPE} is the molecular area of pure DPPE at 3 mN/m, X_{CH} is the mole fraction of cholesterol in the mixture, and A_{CH} is the molecular area of pure cholesterol at 3 mN/m. Using $A'_{DPPE/CH}$ and $A_{DPPE/CH}$, the condensing effect of cholesterol is quantified by determining

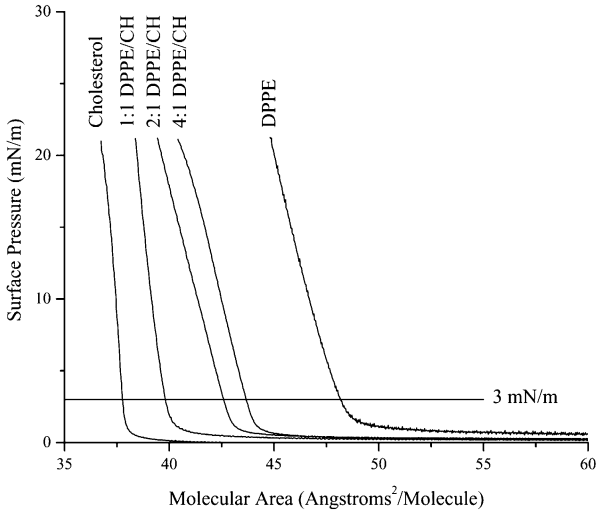

Figure 1. Surface pressure versus molecular area isotherms at room temperature of DPPE, 4:1 DPPE/CH, 2:1 DPPE/CH, 1:1 DPPE/CH, and cholesterol.

Table 1. Actual Average Molecular Area Observed at 3 mN/m (Using an Average of at Least Three Isotherms), the Calculated Ideal Average Molecular Area of Each of the Mixtures, and the Percent Difference between the Two Areas for Each of the Mixtures

sample	actual area (Å²/molecule)	calculated area (Å²/molecule)	percent difference
cholesterol	38		
DPPE	48		
4:1 DPPE/CH	43	46	−7
2:1 DPPE/CH	41	45	−9
1:1 DPPE/CH	39	43	−8

the percent difference of the two molecular areas by the following equation:

$$\text{PercentDifference}(\%) = 100\% \times \frac{A_{DPPE/CH} - A'_{DPPE/CH}}{A'_{DPPE/CH}} \quad (2)$$

Instrumentation. An imaging time-of-flight secondary ion mass spectrometer equipped with a 15 keV Ga^+ liquid metal ion gun (Ionoptika, Southampton, U.K.) was used to obtain mass spectrometric data. The mass spectrometer is described in detail by Braun et al.[16] Spectra were acquired at room temperature without the need for charge compensation and with an ion dose no greater than 10^{12} ions/cm². A total ion image of the analyzed area was obtained by rastering the ion beam across the surface and taking a mass spectrum at each pixel. Topographical AFM (Digital Instruments, Santa Barbara, CA) was performed in tapping mode with a silicon tip (Nano Devices, Santa Barbara, CA) with a force constant of ~40 N/m at a scan rate of 1 Hz.

Results and Discussion

Cholesterol condenses DPPE. Surface pressure versus molecular area isotherms of DPPE, 4:1 DPPE/CH, 2:1 DPPE/CH, 1:1 DPPE/CH, and cholesterol are shown in Figure 1. The condensing effect of cholesterol on DPPE can be seen more clearly from the data in Table 1. The data include the actual average molecular area observed at 3 mN/m for each of the monolayers, the calculated ideal average molecular area for each mixture, and the percent difference between the two areas for each of the mixtures. The average molecular area at 3 mN/m of the different

(13) Fisher, G. L.; Hooper, A. E.; Opila, R. L.; Allara, D. L.; Winograd, N. *J. Phys. Chem. B* **2000**, *104*, 3267−3273.
(14) McConnell, H. M.; Radhakrishnan, A. *Bichim. Biophys. Acta* **2003**, *1610*, 159−173.
(15) Cadenhead, D. A.; Mueller-Landau, F. *J. Colloid Interface Sci.* **1980**, *78*, 269−270.
(16) Braun, R. M.; Blenkinsopp, P.; Mullock, S. J.; Corlett, C.; Willey, K. F.; Vickerman, J. C.; Winograd, N. *Rapid Commun. Mass Spectrom.* **1998**, *12*, 1246−1252.

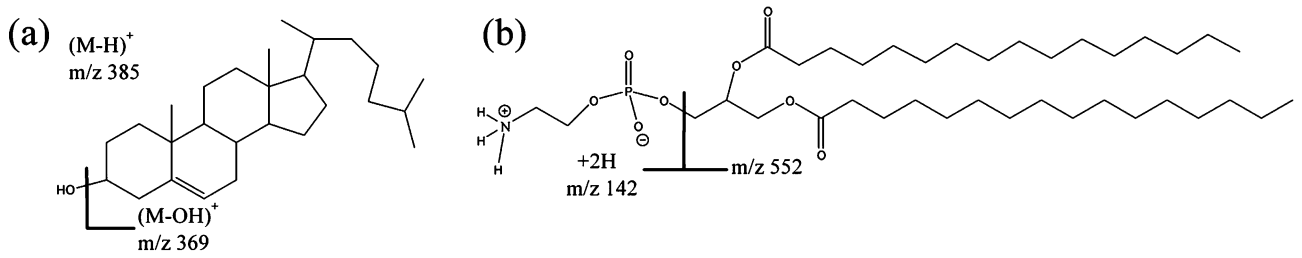

Figure 2. Molecular structures of (a) cholesterol and (b) DPPE shown with the positive SIMS fragment ions of interest labeled. For cholesterol the key fragment ions are $(M-H)^+$ at *m/z* 385 and $(M-OH)^+$ at *m/z* 369. For DPPE the key fragment ions are the tailgroup fragment ion $(C_{35}H_{67}O_4)^+$ at *m/z* 552, the headgroup fragment ion $(C_2H_9PO_4N)^+$ at *m/z* 142, and its dehydration product at *m/z* 124.

monolayers was taken from the average of at least three isotherms. A negative deviation between the actual molecular area and the ideal indicates condensation,[15] and the average percent difference of the two molecular areas examined here is −8%. Thus, it appears that cholesterol condenses DPPE.

We have previously shown that a 2:1 dipalmitoylphosphatidylcholine (DPPC)/CH monolayer results in a −30% difference between the actual molecular area and the ideal;[2] therefore the addition of cholesterol condenses DPPE less than DPPC. As DPPE and DPPC have the same tailgroup, the variance in the condensing ability of cholesterol must be due to the difference in the phospholipid headgroups. The DPPE headgroup has three hydrogens at the N-terminus, whereas the DPPC headgroup has three methyl groups. The size and nature of the DPPE headgroup allow for interheadgroup hydrogen-bonding and thus result in strong DPPE−DPPE interactions[17,18] that encourage DPPE to pack more tightly together at 3 mN/m than DPPC. ToF-SIMS and AFM are used to further understand how the condensation of DPPE by cholesterol influences the monolayer.

Addition of cholesterol to DPPE creates a condensed complex DPPE/CH phase. Chemical identification of the lateral heterogeneity of lipid LB monolayers can be carried out with ToF-SIMS. The molecular structures of DPPE and cholesterol are shown in Figure 2 with the main mass fragment ions labeled. The specific ToF-SIMS peaks that can be used to identify DPPE occur at mass-to-charge ratio (*m/z*) 142 (headgroup fragment ion, $(C_2H_9PO_4N)^+$), *m/z* 124 (dehydration product), and *m/z* 552 (tailgroup fragment ion, $(C_{35}H_{67}O_4)^+$). Cholesterol is identified by the fragment ions $(M-OH)^+$ at *m/z* 369 and $(M-H)^+$ at *m/z* 385. The DPPE fragment ions at *m/z* 124 and *m/z* 142 are not solely specific to DPPE because there are many cholesterol fragment ions between *m/z* 110 and *m/z* 150, and therefore *m/z* 124 and *m/z* 142 cannot be used to map the position of DPPE in the SIMS images.[12] The mass spectra for each of the three mixed monolayers (4:1 DPPE/CH, 2:1 DPPE/CH, and 1:1 DPPE/CH) are shown in Figure 3. Representative mass peaks for each of the lipids, as well as the Au substrate, are apparent in each of the spectra. The relative intensities of the characteristic peaks will be discussed in more detail later.

The SIMS total ion image and the ion images of Au^+ (*m/z* 197), DPPE (*m/z* 552), and cholesterol (*m/z* 369 and *m/z* 385) are presented in Figure 4 for each of the three films. The SIMS total ion images (Figure 4) show that lateral heterogeneity exists for films with less than 50 mol % cholesterol and a homogeneous film for the 1:1 DPPE/CH system. The Au^+ ion images also show that

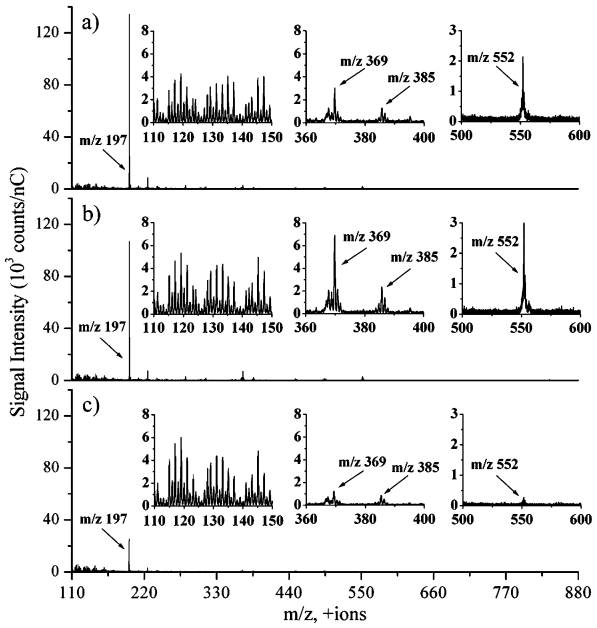

Figure 3. The mass spectra of (a) 4:1 DPPE/CH, (b) 2:1 DPPE/CH, and (c) 1:1 DPPE/CH. The characteristic secondary ions are Au^+ at *m/z* 197, DPPE tailgroup fragment ion $(C_{35}H_{67}O_4)^+$ at *m/z* 552, and cholesterol $(M-OH)^+$ at *m/z* 369 and $(M-H)^+$ at *m/z* 385. The 15 keV Ga^+ ion dose is 10^{12} ions/cm^2 analyzed over an area of 250 μm × 250 μm.

slight heterogeneity exists for the films with less than 50 mol % cholesterol, which will be discussed later in more detail. For each of the films, the DPPE fragment ion images show that DPPE is uniformly present. For the films with less than 50 mol % cholesterol, the cholesterol fragment ion images show micrometer-size cholesterol-rich regions. Each of the DPPE/CH supported LB monolayers was also imaged topographically by AFM (Figure 5). Similar to the SIMS images, the AFM images show that the DPPE/CH films with low cholesterol concentrations are heterogeneous (in height) whereas the 1:1 DPPE/CH film is homogeneous. The heterogeneity of the 4:1 DPPE/CH and 2:1 DPPE/CH LB monolayers indicates the existence of at least two coexisting immiscible phases: a DPPE phase and a DPPE/CH phase. The homogeneous 1:1 DPPE/CH film consists of a single DPPE/CH phase. It is clear from the ToF-SIMS images that DPPE and cholesterol are not segregating within the monolayer; rather a DPPE/CH phase forms and grows. The DPPE/CH phase begins as islands in a connected DPPE phase (4:1 DPPE/CH) that, as the concentration of cholesterol is increased, connect to separate the DPPE phase at the percolation threshold. The DPPE/CH phase continues to grow with addition of cholesterol (2:1 DPPE/CH), and at 50 mol % cholesterol a single homogeneous liquid phase of DPPE/CH is formed.

(17) McMullen, T. P. W.; Lewis, R. N. A. H.; McElhaney, R. N. *Biochim. Biophys. Acta* **1999**, *1416*, 119−134.
(18) Ohvo-Rekila, H.; Ramstedt, B.; Leppimaki, P.; Slotte, J. P. *Prog. Lipid Res.* **2002**, *41*, 66−97.

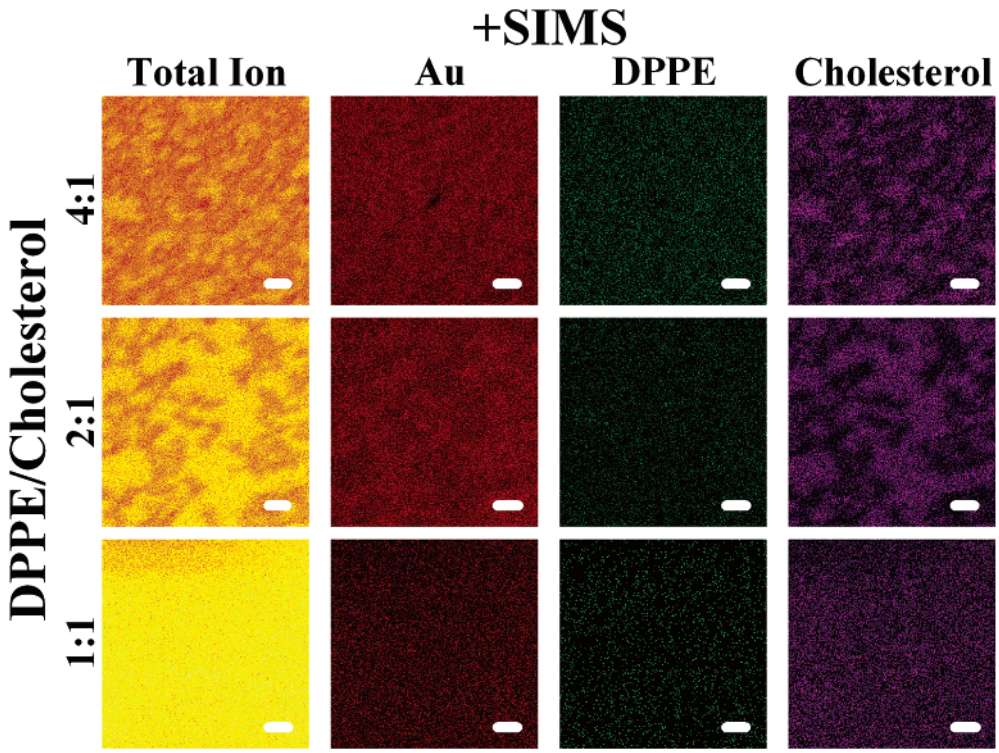

Figure 4. Three DPPE/cholesterol LB films imaged by ToF-SIMS. The images are 256 pixels × 256 pixels with 20 shots/pixel. The 15 keV Ga^+ ion dose is 10^{12} ions/cm^2, and the field of view is 250 μm × 250 μm with the scale bars representing ~40 μm. Au^+ (*m/z* 197) signal is represented in red, DPPE (tailgroup fragment ion $(C_{35}H_{67}O_4)^+$, *m/z* 552) signal is represented in green, and cholesterol ($(M-OH)^+$ *m/z* 369 and $(M-H)^+$ *m/z* 385) signal is represented in purple.

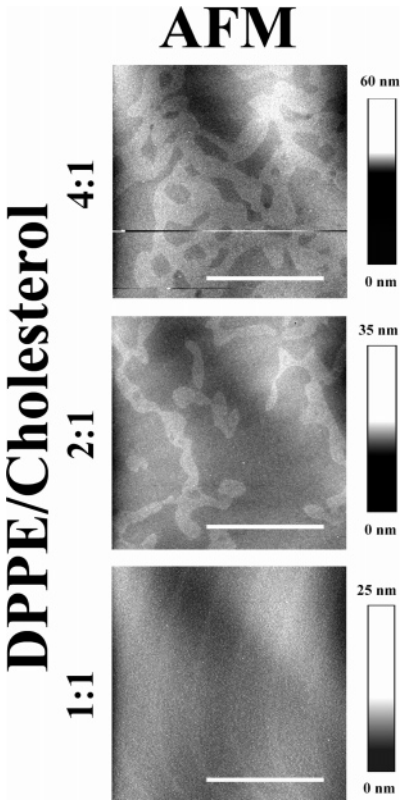

Figure 5. Three DPPE/cholesterol LB films were imaged topographically by AFM. The images are 512 pixels × 512 pixels with a scan rate of 1 Hz. The field of view is 50 μm × 50 μm with the scale bars representing ~25 μm.

The addition of cholesterol to DPPE not only results in the condensation of the DPPE molecules as found in the surface pressure versus molecular area isotherms but also results in the formation of micrometer-size regions of a DPPE/CH phase as determined by ToF-SIMS imaging.

This DPPE/CH phase most likely consists of a cholesterol-DPPE condensed complex. Radhakrishnan and McConnell[19] proposed that the condensing effect of cholesterol results from the reaction of cholesterol and phospholipid to form a condensed complex (P_nC_m). The formation of the condensed complex is evidenced by the existence of two upper miscibility critical points in the surface pressure versus percent cholesterol phase diagram.[19] The critical miscibility region is the maximum surface pressure at which multiple immiscible phases are visible, and the upper miscibility critical point is the maxima of the critical miscibility region.[19] Phospholipids that form condensed complexes with cholesterol have two such immiscibility regions (α and β) and therefore have two upper miscibility critical points.[19] The relative stoichiometry of the condensed complex (*n*:*m*) is determined from the position of the cusp between the two different immiscibility regions, α and β.[19] DPPE should form condensed complexes with cholesterol because dilauroylphosphatidylethanolamine forms condensed complexes with cholesterol and condensed complexes are more likely to form with long-chain saturated lipids.[20] Also, the shape of the DPPE/CH phase in our heterogeneous monolayers (as imaged by AFM in Figure 5) is similar to the "stripe" phase that is indicative of being near, yet below the critical pressure region of two immiscible liquid phases.[21,22] If DPPE and cholesterol form a condensed complex, then it would be the DPPE/CH phase as only one cholesterol-containing phase is observed. Assuming

(19) Radhakrishnan, A.; McConnell, H. M. *J. Am. Chem. Soc.* **1999**, *121*, 486−487.
(20) Keller, S. L.; Radhakrishnan, A.; McConnell, H. M. *J. Phys. Chem. B* **2000**, *104*, 7522−7527.
(21) Seul, M.; Chen, V. S. *Phys. Rev. Lett.* **1993**, *70*, 1658−1661.
(22) Keller, S. L.; Pitcher, W. H., III; Huestis, W. H.; McConnell, H. M. *Phys. Rev. Lett.* **1998**, *81*, 5019−5022.

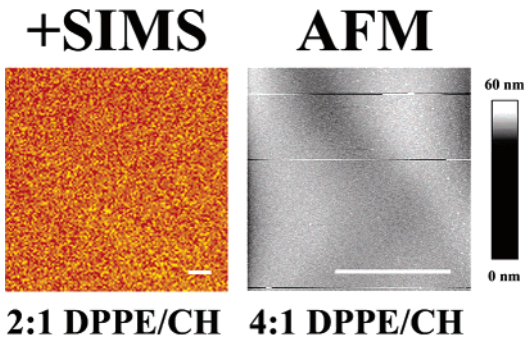

Figure 6. The ToF-SIMS image (the 15 keV Ga^+ ion dose is 10^{11} ions/cm^2 analyzed over a field of view of 250 μm × 250 μm, 128 pixels × 128 pixels with 5 shots/pixel) of the 2:1 DPPE/CH LB monolayer sample substrate. The AFM topography image (50 μm × 50 μm, 512 pixels × 512 pixels with a scan rate of 1 Hz) of the substrate of the 4:1 DPPE/CH LB monolayer sample. The scale bars represent ~25 μm.

DPPE and cholesterol form a condensed complex and that the 1:1 DPPE/CH system is at the cusp, then the stoichiometry of the condensed complex for DPPE and cholesterol should be P_1C_1. These condensed complexes have similar characteristics to the l_o phase found in bilayers that are associated with lipid domains.[22]

The sample substrate does not cause lateral heterogeneity. Several studies have been conducted to compare the lipid monolayer at the air−water interface to the supported lipid LB monolayer and little difference is observed.[9,10] During the deposition of our LB monolayers, a portion of the substrate did not enter the air−water interface so it was left clean of any lipid. This lipid-free portion of the substrate was analyzed simultaneously with the LB lipid monolayer. The SIMS image of the 2:1 DPPE/CH LB monolayer substrate was found to be uniform in intensity (Figure 6). The AFM image of the 4:1 DPPE/CH LB monolayer substrate shows a substrate that is uniform in height (Figure 6). Previously published work,[9,10] the uniformity of the substrates, and the fact that a homogeneous DPPE/CH phase is reached (at 50 mol % cholesterol) all support the hypothesis that the substrate is not the instigator of lateral heterogeneity, but rather the formation of the micrometer-size cholesterol-rich regions is due to the nature of the interacting lipids.

Cholesterol influences the SIMS signal. Using the mass spectra shown in Figure 3, the influence of both cholesterol and the molecular packing on the various ToF-SIMS fragment ion signals can be investigated. The isotherms of the monolayers (Figure 1) demonstrate that the average molecular area of the films decreases with increasing cholesterol concentration. The mass spectra (Figure 3) illustrate that the ratio of DPPE signal (*m/z* 552) to cholesterol signal (*m/z* 369 and *m/z* 385) decreases with increasing cholesterol concentration: 0.6, 0.4, and 0.1 for the 4:1, 2:1, and 1:1 DPPE/CH monolayers, respectively. These ratios indicate that the amount of DPPE detected relative to that of cholesterol is decreasing. In addition, the degree of molecular fragmentation of both lipids (indicated by the mass range *m/z* 110−150) increases with increasing cholesterol concentration (increasing molecular density); thus the closer together the lipids are to one another the more they are prone to fragmentation during primary ion bombardment. This is reasonable because the tighter the molecules are packed, the stronger the molecular interactions and the harder it is for them to be sputtered.

Another interesting feature is that the increase in molecular density from the addition of cholesterol results

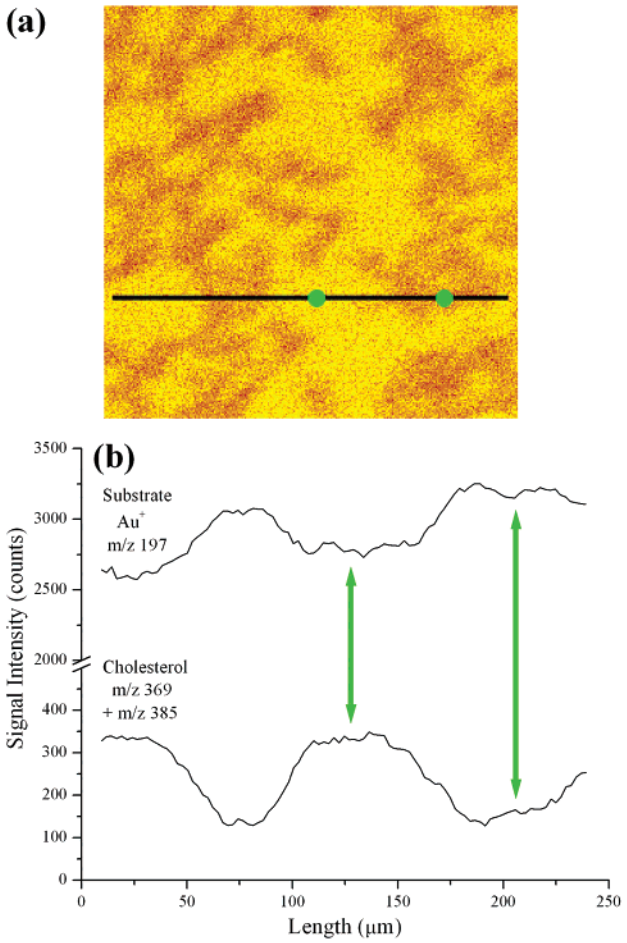

Figure 7. (a) The 250 μm × 250 μm SIMS total ion image of the 2:1 DPPE/CH LB monolayer shown in Figure 4. The 15 keV Ga^+ ion dose is 10^{12} ions/cm^2 with 256 pixels × 256 pixels and 20 shots/pixel. The black line indicates the region selected for the linescan. (b) Linescans taken from the secondary ion images of Au^+ (*m/z* 197) and cholesterol (*m/z* 369 and *m/z* 385) of image a. The secondary ion images are shown in Figure 4. The Au^+ and cholesterol have opposite trends: the Au^+ signal is higher in less dense (less cholesterol) regions and lower in more dense (more cholesterol) regions.

in a decrease in the ToF-SIMS substrate (Au^+) signal. Figure 7 shows a SIMS linescan taken from the secondary ion images of Au^+ (*m/z* 197) and cholesterol (*m/z* 369 and *m/z* 385) of the 2:1 DPPE/CH LB monolayer in Figure 4. The Au^+ and cholesterol signals have opposite trends indicating that the Au^+ signal is higher in less dense (low cholesterol) regions and lower in more dense (high cholesterol) regions. This is likely due to the fact that as molecular area is decreased there is a higher probability for the bombarding projectile or secondary ions to be scattered in the near surface region, thus decreasing the substrate ion signal.

Unfortunately, factors including the addition of cholesterol and the molecular packing make the quantification of SIMS data difficult. Issues related to the quantification of SIMS data resulting from the molecular environment or "matrix effect" have been discussed a great deal.[12,23−28] Ideally, SIMS molecular linescans could be used to determine the percent of the various compounds at

(23) Thompson, P. M. *Anal. Chem.* **1991**, *63*, 2447−2456.
(24) Li, J.-X.; Gardella, J. A., Jr. *Anal. Chem.* **1994**, *66*, 1032−1037.
(25) Li, J.-X.; Gardella, J. A., Jr.; McKeown, P. J. *Appl. Surf. Sci.* **1995**, *90*, 205−215.
(26) Delcorte, A.; Bertrand, P. *Surf. Sci.* **1998**, *412/413*, 97−124.

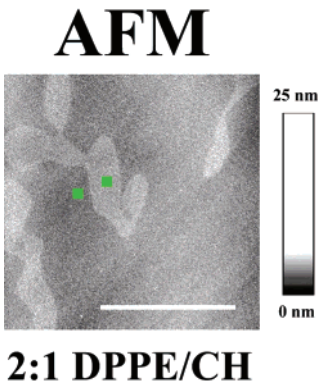

Figure 8. A 25 μm × 25 μm topographic AFM image of the 2:1 DPPE/CH LB monolayer (512 pixels × 512 pixels with a scan rate of 1 Hz). To determine the average height difference between the thick (bright) and thin (dark) regions, localized depth analysis was performed for pairs of 1 μm^2 areas (indicated by green squares). The average height difference between the DPPE (bright) and DPPE/CH (dark) regions is 0.85 nm and was calculated from the average of 20 different pairs. The scale bar represents ~13 μm.

different points across the surface. These studies show that exact quantification of the sample cannot be determined, but rather proportions can be deduced, and the existence and location can be established. These results emphasize the importance of model systems when attempting to interpret ToF-SIMS results of complex systems.

The DPPE phase is thicker than the DPPE/CH phase. A closer investigation of the AFM images (Figure 5) shows that as the amount of cholesterol in the monolayer is increased the fraction of surface area covered by the thick (bright) phase is reduced. From this it can be deduced that cholesterol is in the thinner phase, and from the ToF-SIMS images it is clear that this phase is the DPPE/CH phase; therefore the DPPE phase is the thicker phase. An AFM image of 2:1 DPPE/CH (Figure 8) has an average difference between the DPPE and DPPE/CH phases of 0.85 nm.

The decrease in height upon the addition of cholesterol to DPPE is striking, because the lipids in the DPPE/CH (thinner) phase are more tightly packed than those of the DPPE (thicker) phase. The exact cause for the decrease in height cannot be determined from these data but can reasonably be attributed to the fluidization of the DPPE molecules upon the addition of cholesterol. The isotherm of pure DPPE (Figure 1) indicates it is in a liquid condensed (LC) state at 3 mN/m. The addition of cholesterol is known to change LC phase lipid to a more fluid state.[15] This increased fluidity could result in either a bending or a change in the tilt of the DPPE chains when packed with cholesterol (see Figure 9). Even if the acyl chains of DPPE bend, the DPPE/CH phase is still relevant to the l_o phase of lipid domains because it should be the condensed complex. A change in the tilt of the DPPE molecules upon condensation with cholesterol is not unlikely because the addition of cholesterol is known to do so for DPPC.[29,30] An investigation of the LB lipid monolayers using infrared spectroscopy might be able to distinguish between a bending or tilting of the DPPE chains.

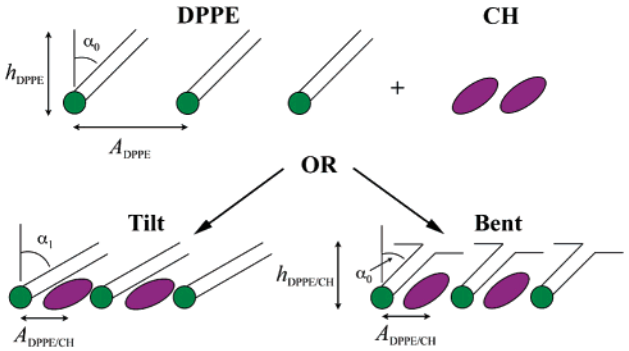

Figure 9. A characterization of two possible reasons for the thinner DPPE/CH phase. A monolayer of pure DPPE has a given molecular area (A_{DPPE}), height (h_{DPPE}), and tilt (α_0). The DPPE/CH phase has a decreased molecular area ($A_{DPPE/CH}$) and is lower in height ($h_{DPPE/CH}$). The decrease in height could be a result of a larger tilt (α_1) or a bending of the acyl chains of DPPE.

The observation of a thinner cholesterol-rich phase for DPPE is also surprising. This is because studies of DPPC and cholesterol LB films found that the regions containing cholesterol are thicker than the pure DPPC regions.[7,30] The actual average molecular area observed at 3 mN/m for the homogeneous 1:1 DPPE/CH monolayer is less than that for a homogeneous 2:1 DPPC/CH monolayer.[2] This higher molecular density forces the molecules closer together and could increase hydrophobic interactions between the acyl chains of DPPE, thus possibly changing the tilt of the packing or bending the chains of DPPE. The decreased thickness of the DPPE/CH phase could aid in transport and signaling across the bilayer, because thinner DPPE/CH regions in the inner leaflet may couple with DPPC/CH regions in the outer leaflet, thus linking the lipid domains across the bilayer. This is another interesting result that emphasizes how small changes in molecular structure, such as different headgroups, can lead to dramatic differences in film architecture.

Conclusion

The lateral heterogeneity of LB films of DPPE and cholesterol was investigated using imaging ToF-SIMS and AFM. Cholesterol was found to have a condensing effect on DPPE that results in lateral heterogeneity of the LB monolayer at low cholesterol concentrations. A 4:1 DPPE/CH film contains micrometer-size islands of DPPE/CH phase surrounded by a DPPE phase. These DPPE/CH regions grow with increasing cholesterol concentration and cross the percolation threshold before 2:1 DPPE/CH, and at 50 mol % cholesterol a single homogeneous liquid DPPE/CH phase exists. Upon the addition of cholesterol, ToF-SIMS lipid characteristic ion and substrate signals are reduced due to the increase in the molecular density of the monolayer. AFM data demonstrate that the DPPE/CH phase is thinner than the DPPE phase. These results have implications for understanding the function of lipid domains in the inner leaflet of cells as phosphatidylethanolamine-lipids are predominant in that leaflet. Thinner DPPE/CH regions in the inner leaflet might match up with DPPC/CH regions in the outer leaflet coupling the cholesterol domains across the lipid bilayer of cellular membranes and enabling molecular transport or signal transduction.

Acknowledgment. Financial support is from the National Institutes of Health and the National Science

(27) Bourdos, N.; Kollmer, F.; Benninghoven, A.; Sieber, M.; Galla, H.-J. *Langmuir* **2000**, *16*, 1481−1484.
(28) Roddy, T. P.; Cannon, D. M., Jr.; Ostrowski, S. G.; Ewing, A. G.; Winograd, N. *Anal. Chem.* **2003**, *75*, 4087−4094.
(29) Smondyrev, A. M.; Berkowitz, M. L. *Biophys. J.* **1999**, *77*, 2075−2089.
(30) Kim, K.; Kim, C.; Byun, Y. *Langmuir* **2001**, *17*, 5066−5070.

Foundation. The authors acknowledge Dr. David L. Allara and his research group for substrate preparation and for the use of their ellipsometer and atomic force microscope. We also thank his research group for their knowledge, expertise, and general willingness to help, especially Tad Daniels, Christine McGuiness, and Josh Stapleton. The authors also thank Juan Cheng, Jason Monnell, and James B. Watney for valuable discussions.

LA0479455